NASA TECHNICAL MEMORANDUM

NASA TM X-3210

NASA TM X-3210

COLD-FLOW ACOUSTIC EVALUATION OF A SMALL-SCALE, DIVERGENT, LOBED NOZZLE FOR SUPERSONIC JET NOISE SUPPRESSION

Ronald G. Huff and Donald E. Groesbeck

Lewis Research Center

Cleveland, Ohio 44135

NATIONAL AERONAUTICS AND SPACE ADMINISTRATION • WASHINGTON, D. C. • MARCH 1975

1. Report No.	2. Government Accession No.	3. Recipient's Catalog No.
NASA TM X-3210		

4. Title and Subtitle	5. Report Date
COLD-FLOW ACOUSTIC EVALUATION OF A SMALL-SCALE, DIVERGENT, LOBED NOZZLE FOR SUPERSONIC JET NOISE SUPPRESSION	March 1975
	6. Performing Organization Code
7. Author(s)	8. Performing Organization Report No.
Ronald G. Huff and Donald E. Groesbeck	E-8153
	10. Work Unit No.
9. Performing Organization Name and Address	505-03
Lewis Research Center National Aeronautics and Space Administration Cleveland, Ohio 44135	11. Contract or Grant No.
	13. Type of Report and Period Covered
12. Sponsoring Agency Name and Address	Technical Memorandum
National Aeronautics and Space Administration Washington, D.C. 20546	14. Sponsoring Agency Code

15. Supplementary Notes

16. Abstract

A supersonic jet noise suppressor was tested with cold flow for acoustic and thrust characteristics at nozzle- to atmospheric-pressure ratios of 1.5 to 4.0. Jet noise suppression and spectral characteristics of the divergent, lobed, suppressor (DLS) nozzle with and without an ejector are presented. Suppression was obtained at nozzle pressure ratios of 2.5 to 4.0. The largest, maximum-lobe, sound pressure level suppression with a hard-wall ejector was 14.6 decibels at a nozzle pressure ratio of 3.5. The thrust loss was 2 percent. In general, low-frequency jet noise was suppressed, leaving higher frequencies essentially unchanged. Without the ejector the nozzle showed a thrust loss of 11 percent together with slightly poorer noise suppression.

17. Key Words (Suggested by Author(s))	18. Distribution Statement
Divergent, lobed suppressor; Acoustics; Acoustic attenuation; Aircraft noise; Jet aircraft noise; Jet exhaust; Jet nozzles; Supersonic nozzles; Suppressors; Noise	Unclassified - unlimited STAR category 71 (rev.)

19. Security Classif. (of this report)	20. Security Classif. (of this page)	21. No. of Pages	22. Price*
Unclassified	Unclassified	40	$3.75

* For sale by the National Technical Information Service, Springfield, Virginia 22151

COLD-FLOW ACOUSTIC EVALUATION OF A SMALL-SCALE, DIVERGENT, LOBED NOZZLE FOR SUPERSONIC JET NOISE SUPPRESSION

by Ronald G. Huff and Donald E. Groesbeck

Lewis Research Center

SUMMARY

A small-scale model of a supersonic jet noise suppressor was tested for its acoustic and thrust characteristics in a cold-flow facility at nozzle- to atmospheric-pressure ratios of 1.5 to 4.0. The acoustic tests were made to determine the jet noise suppression and spectral characteristics of a divergent, lobed, suppressor (DLS) nozzle both with and without a flight-type ejector. These results were compared with those of a circular, convergent nozzle. Thrust data for the DLS nozzle were also taken and compared with the circular-convergent-nozzle data.

Jet noise suppression with the DLS nozzle was obtained at and above nozzle pressure ratios of 2.5. The largest, maximum-lobe, sound pressure level suppression was 14.6 decibels at a nozzle pressure ratio of 3.5. The thrust loss was 2 percent with the ejector installed. Sideline attenuation was 10 decibels at these conditions. Suppression was obtained at the lower frequencies, with the higher frequencies essentially unchanged. Without the ejector a thrust loss of 11 percent was obtained with the DLS nozzle.

INTRODUCTION

Future commercial aircraft may fly faster than current aircraft but will be required to meet community noise standards set by regulating government agencies. The turbojet or high-pressure-ratio bypass fan engine offers an efficient powerplant for future high-speed aircraft, provided the high-velocity jet noise associated with such engines can be suppressed to an acceptable level when the aircraft is operating at low altitudes near the airport.

In selecting an engine for installation in future aircraft, many factors such as thrust, engine weight, and nacelle drag must be explored, and a compromise must be reached that will yield the best applicable engine. Factors determining direct operating cost, such as specific fuel consumption, are also important. Engines with small cross sections, such as turbojets, will require high jet velocities to provide the necessary thrust. The noise generated by the jet is dependent on the jet velocity with an exponent between 3 and 8 (refs. 1 and 2), depending on the jet velocity and pressure ratio. Thrust, on the other hand, is a function of both weight flow rate and the jet velocity to the first power.

From the noise standpoint, reducing the jet velocity results in large reductions of jet noise so that the trend is to build larger engines having lower jet velocities to minimize jet noise and having larger airflow rates to maintain the required thrust. However, smaller engines of equal thrust offer decreased drag and weight. Since drag increases with the square of the aircraft velocity, it may be desirable for high-velocity aircraft to use smaller engines with high jet velocities to obtain the required thrust. Jet noise suppressors will then be necessary. A number of jet noise suppressors have been devised and tested. A summary of several types is given in reference 3.

A new device for reducing supersonic jet noise is shown in figure 1 and was reported in references 4 and 5. The suppressor is similar to a convergent-divergent nozzle in that the circular, convergent nozzle has a divergent, lobed section attached to it. This divergent, lobed, suppressor (DLS) nozzle uses strong internal shocks to reduce the jet velocity. The aerodynamics of the DLS nozzle flow and some gross noise measurements are contained in reference 4. The effects of various geometric variations of the DLS nozzle on the thrust loss and the largest, maximum-lobe, noise suppression are given in reference 5. Maximum-lobe, noise suppression of 15 decibels and a thrust loss of 2.5 percent with an ejector installed were reported. The noise measurements for the data reported in references 4 and 5 were made with a hand-held portable sound meter and did not yield detailed sound data. In order to obtain more detailed acoustic data on the DLS nozzle with and without an ejector, the best small-scale configuration of references 4 and 5 was tested in a cold-flow jet noise facility at the NASA Lewis Research Center. Thrust data for these configurations were taken by using a cold-air thrust stand. The detailed acoustic and thrust data are presented in this report.

The circular, convergent nozzle (throat diameter, 7.62 cm) used for the tests reported in references 4 and 5 was fitted with the DLS nozzle described in the apparatus section of this report. The air temperature was approximately 280 K, and the nozzle pressure ratio was varied from 1.5 to 4.0. Jet noise suppression was obtained at and above a nozzle pressure ratio of 2.5. Thrust loss is presented by using the theoretical thrust of the circular, convergent nozzle as the reference nozzle value. Representative sound pressure level (SPL) and sound power level (PWL) spectra are presented. The measured, total, jet noise, acoustic power level is compared with that calculated by the method reported in reference 2 for both the circular, convergent nozzle and the circular, convergent nozzle with the DLS nozzle installed. The symbols used in this report are defined in appendix A.

The work presented herein was done in the U.S. customary system of units. Conversion to the International System of Units (SI) was for reporting purposes only.

SUPPRESSOR DESCRIPTION AND OPERATION

A detailed description of the divergent, lobed, suppressor nozzle is given in reference 4. A brief summary of the description and operation of the suppressor is given here to aid the reader in understanding the aerodynamics of the divergent, lobed, suppressor (DLS) nozzle.

The suppressor uses the pumping action of the jet leaving a circular, convergent (primary) nozzle on a base cavity to create a low-pressure region in a diverging multilobed passage downstream of the primary nozzle exit (figs. 1 and 2). The base cavity pressure is much lower than ambient pressure. The low pressure causes the flow to overexpand and fill the divergent, lobed section of the nozzle. The overexpansion results in a higher supersonic Mach number than would have resulted from a free expansion of the air from the convergent nozzle to ambient pressure. In supersonic flow the higher the Mach number of the flow, the stronger is the shock. A system of strong shocks exists in the divergent, lobed section of the nozzle because of the turning of the supersonic flow at the nozzle wall and the necessary adjustment of the jet static pressure to ambient pressure. This shock system results in a more rapid decrease in the jet Mach number, and hence velocity, downstream of the shock than exists for the flow from a circular, convergent nozzle operating at an identical nozzle pressure ratio P_N/p_0. The resulting lower jet velocity yields less noise than does the circular, convergent nozzle because of the noise dependence on the third to eighth power of the jet velocity.

An additional noise benefit may result from the splitting of the flow between the lobes in the divergent section of the nozzle. The multipeaked jet velocity profiles of the DLS nozzle (ref. 4) create a flow pattern similar to those of multitube jet noise suppressors in current use. Shielding of the inner jets by the outer jets decreases the noise emitted to the far-field observer (ref. 6).

APPARATUS

Geometry of Divergent, Lobed, Suppressor Nozzle

The basic configuration selected from those reported in references 4 and 5 for detailed acoustic study was that listed in reference 5 as configuration 6-V(0.75). An isometric drawing of this configuration is shown in figure 2(a); dimensions are given in figure 2(b). The basic configuration consisted of a circular, convergent nozzle with a divergent, lobed section added at the throat station. The basic configuration had a primary-plate divergence angle of 15°, a circular convergent (primary) nozzle throat diameter D_t of 7.62 centimeters, a ratio of base cavity step height to circular-convergent-nozzle throat diameter h/D_t of 0.042, a ratio of V-shaped gutter plate length to nozzle throat diameter of 0.75, and a ratio of primary-plate length to nozzle throat diameter of 0.917. The ejector had a constant inside diameter ($D_e/D_t = 2.0$) and an airfoil-shaped inlet lip. It was considered to be representative of flight hardware. The ratio of the length of the test ejector to the nozzle throat diameter was 2.44. The axial position of the ejector was varied to determine the optimum position for the perceived noise level. During most of the testing the ejector was positioned in the axial direction so that its leading edge was one nozzle throat diameter ($x/D_t = 1.0$) from the primary nozzle throat axial station. This location was determined from unpublished exploratory NASA data to yield the highest thrust augmentation. The circular, convergent nozzle with the ejector and the divergent, lobed section removed was used to obtain reference data.

Facility and Instrumentation

Figure 3 shows the cold-flow jet noise facility used for the present tests. The air was supplied from a central air supply to the pipe shown in the foreground. The flow rate was controlled by a 15.24-centimeter-diameter, remotely operated globe valve placed in the 20.32-centimeter-diameter pipeline. An internal noise muffler was located just downstream of the valve. This muffler lowered the valve and internal noise to acceptable levels. The air then passed through the 20.32-centimeter-diameter pipe to a reducer. The reducer was used to mate the facility piping to the 15.24-centimeter-diameter-nozzle mounting flange. The piping was located 1.52 meters above the ground plane, with the exit of the test nozzle at the center of the 4.57-meter-radius microphone circle shown in figure 3.

The microphone circle was in a vertical plane that passed through the centerline of the air pipeline. The microphones were mounted on booms extending from a vertical semicircular arc support. The microphones were located at 20°, 40°, 60°, 75°, 90°, 105°, 120°, 135°, 145°, 155°, and 165° angular locations measured from the upstream (inlet) jet axis. Each 1.27-centimeter-diameter condenser microphone was covered by a windscreen. The ground under the microphones was covered with open-cell acoustic foam to minimize ground reflections (fig. 3). The data measured by the microphones were taken to be free-field data above a frequency of 400 hertz (ref. 7). The acoustic data from each microphone were analyzed on line, and the results were recorded on magnetic tape.

Thrust measurements for the DLS nozzle, the DLS nozzle with ejector, and the circular, convergent nozzle were made in the same cold-air thrust stand used for the aerodynamic tests reported in reference 4. Details of the thrust measuring system are given in reference 4. Briefly, the thrust was measured by a load cell mounted at the upstream end of the freely floating nozzle air supply line.

In both the acoustic and thrust measuring facilities the temperature of the cold-air supply was monitored by a thermocouple located in the air supply line. The nozzle inlet total pressure P_N was measured with a pitot tube located just upstream of the nozzle inlet. The acoustic facility made use of a pressure transducer to read the nozzle inlet total pressure, while the thrust measuring facility used a precision Bourdon tube pressure gage to read the nozzle inlet total pressure. The data were taken over a range of nozzle- to atmospheric-pressure ratios P_N/p_0 of 1.5 to 4.0.

DATA REDUCTION

The noise data from each of the microphones were analyzed directly by an automated 1/3-octave-band frequency spectrum analyzer, and the results were recorded on magnetic tape. The analyzer determined the uncorrected sound pressure level (SPL) spectra referenced to 20 micronewtons per square meter. The magnetic tape containing the uncorrected data was processed at a later time by using a computer program. The SPL spectra were corrected for atmospheric attenuation (less than 1 dB). The data as reported are free field above 400 hertz and lossless. The SPL spectra were used to calculate the overall sound pressure level (OASPL). The specific equation used is given in appendix B.

The sound power level (PWL) spectrum was calculated by assuming that the jet noise was symmetrical about the jet axis. A portion of the surface area of a sphere having its center at the test nozzle exit and a radius equal to the microphone circle radius was assigned to each microphone. The surface area segment was bounded by the intersection of two planes passing through the sphere perpendicular to the jet axis and through points on the spherical surface that bisected the angle between adjacent microphones. The PWL was calculated from the SPL spectra by using the equation given in appendix B. The reference power was 10^{-13} watt. The overall sound power level (OAPWL) was calculated by summing the power in watts for each 1/3-octave-band-pass filter over the entire analyzed spectrum and then converting the resulting total power to decibels.

Thrust loss is defined as the difference between the circular, convergent nozzle ideal net thrust $F_{n,th,c}$ and the measured net thrust $F_{n,exp}$ divided by the circular convergent nozzle ideal net thrust $F_{n,th,c}$, converted to a percentage. The equation for the ideal net thrust is given in appendix B.

In all data reductions, the assumption was made that for nozzle pressure ratios P_N/p_0 below choking the static pressure at the throat station was equal to atmospheric pressure. For nozzle pressure ratios above choking the throat static pressure was calculated from the one-dimensional, isentropic, choked-flow equations.

RESULTS AND DISCUSSION

In the following discussion the results of the small-scale, cold-flow noise tests are given with emphasis placed on comparison of the directivity, the sound pressure level spectra, and the overall sound pressure level suppression given by the DLS nozzle with those given by the circular, convergent nozzle. The sound power spectrum for each nozzle pressure ratio is discussed, and the total power given. The thrust loss of the DLS nozzle is discussed, along with the thrust recovery obtained by use of the ejector.

The SPL spectra for nozzle pressure ratios at which noise suppression is obtained are given for the maximum-lobe location and the 90° angular location. In this report the maximum-lobe location is defined as the angular location on the microphone circle at which the maximum overall sound pressure level occurs. Comparisons to the circular convergent nozzle are made for the DLS nozzle with and without the ejector installed. The DLS nozzle suppressed jet noise at and above nozzle pressure ratios P_N/p_0 of 2.5. For lower pressure ratios the flow from the primary nozzle did not attach to the divergent, lobed section of the nozzle; hence, no noise suppression was obtained.

Acoustics

Directivity. - The lossless OASPL of the circular, convergent nozzle, the DLS nozzle, and the DLS nozzle with ejector are shown in figure 4 as a function of the acoustic radiation angle (directivity). The radial distance to each microphone was 4.57 meters. The data shown in figure 4 are for nozzle pressure ratios of 1.5 to 4.0. In figures 4(a) and (b) (pressure ratios 1.5 and 2.0, respectively) the flow has not attached to the primary plates in the divergent, lobed section of the nozzle; and the DLS nozzle produces a noise increase rather than a suppression.

For nozzle pressure ratios between 2.5 and 4.0 the DLS nozzle and the DLS nozzle with ejector are quieter over the entire range of acoustic radiation angles than the circular, convergent nozzle, as shown in figures 4(c) to (f). The attachment of the flow to the divergent, lobed section of the nozzle at these pressure ratios was accompanied by a decrease in the maximum-lobe sound pressure level. Furthermore, the directivity of the DLS nozzle noise became more uniform than that of the circular, convergent nozzle.

In this pressure ratio range the circular, convergent nozzle generated strong tones at pressure ratios of 3.0 and 3.5. These tones are a result of shock oscillation (ref. 8). The data denoted by the marked symbols contain tones. The dominant frequencies were 1600 and 3150 hertz, although at a nozzle pressure ratio of 2.5 a low sound pressure level tone with a 2500-hertz frequency was detected with the 20° microphone. These data have been adjusted for the tones; the tonal SPL was subtracted from the OASPL and the data were replotted in figures 4(d) to (f).

For the DLS nozzle the maximum OASPL occurred at a β of 135° from the inlet axis compared to the 155° angular location for the circular, convergent nozzle. With the ejector installed the maximum-lobe location was less well defined. For these data the ejector was positioned at the optimum axial position ($x/D_t = 1.0$) for thrust augmentation. The ejector wall was not acoustically treated, but the maximum OASPL with the ejector in place was somewhat (1.3 to 3 dB) lower than that for the DLS nozzle alone. The ejector tended to further decrease the directionality of the DLS nozzle noise pattern.

Sound pressure level spectra. - As previously mentioned, the maximum-lobe location is defined as the angular location on the microphone circle where the OASPL is a maximum. The maximum-lobe sound pressure level spectra for the circular, convergent nozzle, the DLS nozzle, and the DLS nozzle with ejector are shown in figure 5. The spectra shown are for nozzle pressure ratios between 2.5 and 4.0 at a microphone distance of 4.57 meters. The maximum-lobe OASPL for each nozzle configuration is given in the key. The spectra for the lower nonsuppression pressure ratios are not shown.

Comparing the spectra for the plain DLS nozzle with those for the circular, convergent nozzle shows that the DLS nozzle suppresses at the lower frequencies (<5000 Hz). At high frequencies (>5000 Hz) the SPL values for the suppressor nozzle with and without ejector were slightly higher than those with the circular, convergent nozzle, particularly at a nozzle pressure ratio of 2.5.

The addition of the ejector to the DLS nozzle reduced the peak SPL data shown in figure 5 throughout the nozzle pressure ratio range of 2.5 to 4.0. At pressure ratios of 3.5 and 4.0 the DLS nozzle with ejector showed an increased low-frequency (<1250 Hz) SPL, and the spectra had two peaks instead of the one exhibited by the lower pressure ratio data. The lower frequency SPL peak (500 Hz) is greater than the higher frequency SPL peak (8000 Hz).

The circular-convergent-nozzle spectra shown in figure 5 generally did not show evidence of tones except at a nozzle pressure ratio of 3.0. The tone for this pressure ratio was generated in the range of the 1600-hertz, 1/3-octave-band-pass filter and was caused by shock wave oscillation (ref. 8).

Ninety degree (ground-level sideline) spectra. - The maximum sideline noise after the SPL at the microphone circle was corrected for the radial distance to the 4.57-meter sideline occurred at a microphone angular location of 90° for pressure ratios greater than 2.0. The sound pressure level spectra for the 90° angular location at a 4.57-meter sideline are shown in figure 6. The spectra are for nozzle pressure ratio conditions that yielded suppression (i.e., P_N/p_0 of 2.5 to 4.0) and are from the same runs as the data shown in figure 5. The plain DLS nozzle, with slight exception at the nozzle pressure ratio of 2.5, had a lower SPL than the circular, convergent nozzle throughout the nozzle pressure ratio range.

The addition of the ejector to the DLS nozzle resulted in slightly increased SPL for the lower frequencies (<1250 Hz). These increases were much less apparent for the 90° SPL than they were for the maximum-lobe SPL (figs. 5(c) and (d)). The higher frequency data either decreased or remained the same. The high frequencies dominated the 90° SPL spectra over the range of pressure ratios where the DLS nozzle suppressed the jet noise.

The circular, convergent nozzle SPL spectra for the sideline (90°) microphone location show distinct tones generated at pressure ratios of 3.0, 3.5, and 4.0. The SPL that were considered to be tone values are denoted in figure 6 by the marked symbols. The indicated tones are generated by the oscillation of the shock wave (ref. 8) and can be removed by disturbing the shock wave pattern, that is, by placing a finger or other obstruction in the flow at one side of the nozzle. These SPL were not used in the calculations of OASPL for the 90° microphone location.

Maximum-lobe suppression. - The maximum-lobe suppression of the suppressor nozzle is defined in this report as the maximum OASPL of the circular, convergent nozzle minus the maximum OASPL of the test configuration obtained from figure 4.

The maximum-lobe OASPL suppression for the DLS nozzle and the DLS nozzle with ejector is shown by the solid lines in figure 7 as a function of the nozzle total pressure ratio. (The dashed lines in fig. 7 giving the ground-level sideline suppression are discussed in the next section of this report.) The largest maximum-lobe suppression occurred at a nozzle pressure ratio of 3.5. For the DLS nozzle alone the largest maximum-lobe suppression was 11.7 decibels; for the DLS nozzle with ejector this suppression was 14.6 decibels. The double points at a pressure ratio of 2.5 are data taken just before and just after jet attachment to the DLS nozzle.

Ninety degree (ground-level sideline) suppression. - An observer located on an aircraft flightpath sideline hears noise that varies in inverse proportion to the square of the distance to the aircraft. The test-stand noise data recorded from each microphone in a circular microphone array must be adjusted for the increase in radial distance to the sideline. The adjustment of the test-stand noise data for sideline locations is a function of the radial distance to the sideline from the microphone and the angular location of the observer. In order to estimate the noise for a real aircraft, the angle of the jet axis to the ground plane, the aircraft altitude, and atmospheric attenuations are required to correct test-stand acoustic data to the real aircraft sideline values. Obtaining these values requires knowledge of the aircraft's operating characteristics and atmospheric conditions and is considered beyond the scope of this report. However, the test-stand data can be adjusted to give representative sideline data at ground level. The lossless OASPL data given in figure 4 were measured at a 4.57-meter-radius arc. If each of the OASPL values was adjusted for the radial distance to the sideline by the inverse square law, the maximum-lobe noise in all the small-scale test data would no longer dominate the sound field. For nozzle pressure ratios greater than 2.0 the 90° microphone location dominated the sideline noise for all nozzles tested. The ground-level sideline noise suppression is defined as the maximum sideline OASPL of the circular, convergent nozzle minus the maximum sideline OASPL of the DLS nozzle configuration. The maximum sideline noise just happened to occur at the 90° angular location. The 90° suppression obtained for the DLS nozzle with ejector is given by the dashed line in figure 7 for a sideline distance of 4.57 meters. The OASPL data used in these calculations had the tones removed before the suppression values were calculated. The data show that the maximum sideline OASPL suppression is 12 decibels at a nozzle pressure ratio of 3.0. The suppression decreases to 8 decibels at a pressure ratio of 4.0, to 10 decibels at a pressure ratio of 3.5, and to 7 decibels at a pressure ratio of 2.5.

Sound power level spectra. - The power spectra for the circular, convergent nozzle, the DLS nozzle, and the DLS nozzle with ejector are shown in figure 8 for the entire range of nozzle pressure ratios reported herein. The OAPWL with tonal PWL value subtracted is given in the key for each configuration.

Figures 8(a) and (b) show the spectra for the lower nozzle pressure ratios (P_N/p_0 of 1.5 and 2.0), at which jet noise suppression did not exist. At these nonsuppression nozzle pressure ratios the shapes of the power spectra for the DLS nozzle and the DLS nozzle with ejector were similar. The dominant PWL was slightly greater for the DLS nozzle with ejector than for the DLS nozzle alone. The DLS-nozzle spectrum, as would be expected from comparison of the total PWL values, was generally higher than the circular-convergent-nozzle spectrum.

The sound power level spectra for the noise-suppression pressure ratios are shown in figures 8(c) to (f). Generally, the DLS nozzle and DLS nozzle with ejector showed a power spectrum dominated by the high frequencies. Addition of the ejector to the DLS nozzle tended to decrease the high-frequency PWL and to increase the PWL at lower frequencies. For example, at a nozzle pressure ratio of 3.5, the SPL spectrum at the maximum-lobe location (fig. 5(c)) showed a dominant low-frequency peak. To a lesser extent the increase in the lower frequency SPL was present at the 90° location (fig. 6(c)). The lower frequency PWL spectra (fig. 8(e)) reflected this lower frequency increase in the sound pressure levels.

The circular-convergent-nozzle PWL spectra exhibited dominant tones at nozzle pressure ratios of 3.0 and 3.5 at frequencies of 1600 and 3150 hertz. The total power, including the tonal PWL, was 159.7 and 161.5 decibels for nozzle pressure ratios of 3.0 and 3.5, respectively. Excluding the tonal PWL yielded total powers of 155.6 and 158.7 decibels for these nozzle pressure ratios.

Total power level. - The total power level (OAPWL) is a gross measure of the amount of noise being generated by the jet. The experimentally determined total power level (OAPWL calculations shown in appendix B) is presented in figure 9 as a function of the predicted, jet noise, total power level of the circular, convergent nozzle. The predicted total power was calculated by the method given in reference 2, with slight modification, and is applicable for both subsonic and supersonic jet noise calculations. The Lighthill constant (ref. 1) used to obtain the jet noise correlation of reference 2 was 3.0×10^{-5}. Other investigators have found Lighthill constants ranging from 2.7×10^{-5} to 5.5×10^{-5} (refs. 9 and 10, respectively). The range of constants accounts for a 3-decibel uncertainty in the jet noise predictions. Using a constant of 3.0×10^{-5} in reference 2 results in underpredicting the circular-convergent-nozzle total power. Because of uncertainty in the constant, and in view of the underprediction of the total power when using a constant of 3.0×10^{-5}, a 3-decibel adjustment has been arbitrarily added to the total power predicted by the method of reference 2. The addition of 3 decibels to the predicted total power simply changes the constant of 3.0×10^{-5} used in reference 2 to 6.0×10^{-5}, thus bringing the predicted total power into better agreement with the experimentally determined total power of the circular, convergent nozzle. The solid line with a 45° slope shown in figure 9 is used for reference purposes. It represents the predicted total power of the circular, convergent nozzle. A second scale on the abscissa shows the nozzle pressure ratio.

A comparison of the total power levels of the circular, convergent nozzle, the DLS nozzle, and the DLS nozzle with ejector is made in figure 9. The data for the circular, convergent nozzle are shown by the circular symbols. At pressure ratios of 3.0 and 3.5, tones appeared in the power spectrum of the circular, convergent nozzle (figs. 8(d) and (e)). These tones dominated the experimentally determined total power level (OAPWL). The experimentally determined total power given in figure 9 for the circular, convergent nozzle has been adjusted by subtracting the contribution of the tonal PWL from the OAPWL. After correcting the data for tones, the PWL for the circular, convergent nozzle at nozzle pressure ratios of 1.5, 3.0, 3.5, and 4.0 appeared to be reasonably predicted by a Lighthill constant of 6.0×10^{-5}. At pressure ratios of 2.0 and 2.5, differences of 2 and 3 decibels, respectively, were found. The jet noise correlation (ref. 2) did not account for convective Mach number effects found near a jet Mach number of 1.0. This may account for the deviation between the predicted and measured PWL at nozzle pressure ratios of 2.0 and 2.5.

The data for the DLS nozzle and the DLS nozzle with ejector showed a large decrease (as much as 12 dB) in the total power level compared to the total PWL of the circular, convergent nozzle for pressure ratios above 2.5. The data follow the general trend shown by the OASPL suppression (fig. 7). The DLS nozzle with the ejector had a lower total sound power level (by 2 dB) than the DLS nozzle alone.

Aeroacoustics

The combination of acoustic and thrust performance of any jet noise suppressor is of prime importance to aircraft powerplant and airframe designers. The designer needs to know both the noise suppression and the thrust loss penalty that must be paid to decrease the aircraft's noise level.

Thrust loss. - Figure 10 compares the thrust losses of the circular, convergent nozzle, the DLS nozzle, and the DLS nozzle with an ejector installed at one primary nozzle throat diameter from the primary nozzle axial throat station. Thrust loss is shown as a function of the nozzle total pressure ratio. The circular-convergent-nozzle thrust loss is given for reference purposes. The thrust loss of the DLS nozzle peaked at a pressure ratio of 2.5 and also was double valued. This was a direct result of the abrupt flow attachment to and detachment from the divergent, lobed section of the nozzle. It is apparent that the thrust loss of the DLS nozzle alone was larger than desirable, but the addition of the ejector decreased the net thrust loss at test-stand conditions.

The maximum-lobe suppression occurred at a nozzle pressure ratio of 3.5, and the thrust loss for the DLS nozzle with ejector became reasonable at and above this pressure ratio.

The thrust loss of the DLS nozzle with ejector at a pressure ratio of 3.5 was 3 percent. The corresponding circular-convergent-nozzle thrust loss was 1 percent. The difference then in thrust loss between the DLS nozzle with ejector and the circular, convergent nozzle is 2 percentage points. At pressure ratios greater than 3.8 the DLS nozzle with ejector gave greater thrust than the circular, convergent nozzle. At a pressure ratio of 4.0 a thrust gain of 0.5 percent above the actual circular-convergent-nozzle thrust was achieved.

Suppression and thrust loss. - The acoustic suppression and thrust loss data are summarized in figure 11, where the acoustic suppression data of figure 7 are plotted as a function of the percent thrust loss given in figure 10. The data shown are for nozzle pressure ratios from 2.5 to 4.0. The maximum-lobe, sound pressure level suppression with the ejector installed at the optimum thrust axial position x/D_t of 1.0 was 14.6 decibels, with a thrust loss of 3 percent from the theoretical thrust. For a thrust loss of 0.4 percent the suppression was 12.8 decibels. Without the ejector the thrust loss for the DLS nozzle was increased, while the suppression was decreased slightly.

The 4.57-meter-sideline sound pressure level suppression with ejector installed was 7.5 decibels with a thrust loss of 0.4 percent. A maximum sideline suppression of 12 decibels was reached with a thrust loss of 8.0 percent.

ESTIMATED PERCEIVED NOISE LEVELS FOR FULL-SIZE NOZZLE

A 357-kilonewton- (80 000-lbf-) thrust engine is assumed to be a reasonable size for use on a supersonic commercial aircraft. An engine of this class would have a circular exhaust nozzle throat diameter of the order of 1 meter, or about 15 times that of the small-scale model test nozzle.

In order to apply the small-scale, cold-flow data when scaling the test data to a full-size engine exhaust nozzle, it is necessary to make two basic assumptions:

(1) The conceptual engine is a high-bypass-ratio turbofan operating with fan pressure ratios between 2.5 and 4.0; the fan flow is relatively cold; and the fan jet noise dominates the noise field.

(2) The core engine jet does not adversely affect the aerodynamics of the DLS nozzle; that is, most of the energy from the core engine is used to drive the fan, leaving a low-energy, low-temperature core exhaust jet.

The data used for the scaling estimation are static, ground-level values. The method used for the scaling estimation is given in appendix C. The effect of temperature on directivity and suppression is discussed in appendix D.

The applicable noise measuring station for a supersonic aircraft is at the 648-meter sideline. The estimated 648-meter-sideline perceived noise levels for a full-size nozzle (D_t = 1.14 m) equal to 15 times the test model size are shown in figure 12 as a function of angular position from the forward jet axis and nozzle pressure ratio. The limit set by FAR-36 (ref. 11) for the assumed aircraft is 108 effective perceived noise decibels (EPNdB) at the 648-meter sideline. The 90° location is dominant for the circular, convergent nozzle, the DLS nozzle, and the DLS nozzle with ejector (figs. 12(a), (b), and (c), respectively). The maximum PNL's for the nozzles are shown on figure 12. The circular-convergent-nozzle PNL's at the 90° location required adjustment to remove the tones that appeared in the small-scale-spectra data (fig. 6). This adjustment was accomplished by substituting SPL values obtained by fairing the spectra and then calculating the perceived noise levels with the faired values of the SPL at the tonal frequencies. From figure 12(a) a single, circular, convergent nozzle creates 108.4 PNdB. If four were required, the sideline PNL would be increased to 114.4 PNdB, exceeding the regulation by 6 PNdB. Use of the DLS nozzle with ejector would reduce the PNL to 106.3 PNdB, or 1.7 PNdB below the regulation. From figure 12 the PNL suppression can be determined by subtracting the suppressor maximum sideline PNL from that of the circular, convergent nozzle.

Figure 13 shows the PNL suppression along a 648-meter sideline for the DLS nozzle alone as a function of nozzle pressure ratio. The suppression is also shown for the DLS nozzle with ejector located at $x/D_t = 1.0$, the optimum thrust position, and at $x/D_t = 1.33$, the best acoustic position. The curves show that the maximum PNL suppression occurred at a nozzle pressure ratio of 3.0. The nominal suppression values ranged from 6 to 13 PNdB depending on pressure ratio and ejector position. The applicability of this information depends on the configuration, size, temperature, pressure, and fan-to-core bypass ratio. Therefore, the specific application is left to the reader.

The effect of ejector axial position on noise suppression was also studied. The hard-wall-ejector axial position was varied over a range of x/D_t ratios from 0 to 1.66 during the small-scale tests. These data were used to determine the full-size nozzle PNL. The maximum PNL as a function of ejector position and nozzle pressure ratio is shown in figure 14 at the 648-meter-sideline location. Ejector axial position had little effect on PNL at nozzle pressure ratios of 2.5 and 4.0. At nozzle pressure ratios of 3.0 and 3.5 the lowest PNL were obtained at an ejector x/D_t of 1.33. The PNL values at this ejector location for these nozzle pressure ratios were 1 to 1.6 PNdB lower than those at the $x/D_t = 1.0$ location used in figure 12. For comparative purposes the PNL of the DLS nozzle alone and the circular, convergent nozzle are included in figure 14.

CONCLUDING REMARKS

In these concluding remarks some speculative comments are made concerning the application of the divergent, lobed, suppressor nozzle to a real engine. The effect of the ejector on the perceived noise, the atmospheric attenuation effects, the additional noise suppression techniques used with the DLS nozzle, and the application of the DLS nozzle to real engines requiring variable-geometry nozzles are discussed.

Effect of Ejector

The maximum sideline noise for the DLS nozzle was dominated by the data from the 90° angular location. The sound pressure level spectra at this location showed little change resulting from the addition of an ejector. The dominance of the 90° angular location on sideline noise may not prevail with a hot jet (appendix D).

If it were assumed that because of aircraft climb angle and/or hot jet temperature the dominance of the sideline noise changes from $\beta = 90^{\circ}$ to the maximum-lobe noise angular location, the effect of the ejector on the sound pressure level spectrum would become important. As shown in figure 5 (the maximum-lobe results) the spectra at nozzle pressure ratios of 3.5 and 4.0 were greatly influenced by the ejector. These spectra must then be considered in light of the weighting given various frequencies in making a perceived noise level calculation. The scaling of these spectra to a full-size nozzle for a 357-kilonewton-thrust engine caused the lower frequency SPL hump to occur at a frequency of approximately 30 hertz. In the PNL calculations, SPL below 500 hertz were suppressed. Therefore, the lower frequency hump in the spectra can be neglected. This low-frequency sound is important for structural reasons; however, that subject is beyond the scope of this report.

The higher frequency SPL hump occurred at about 500 hertz at this engine size. In the PNL calculation the weighting of the SPL at this frequency was negligible. The SPL spectra at the higher frequencies for the DLS nozzle with ejector were lower than those of the circular, convergent, reference nozzle and the DLS nozzle. Thus, it is to be expected that the sideline PNL of the DLS nozzle with ejector might be lower than the sideline PNL at the 90° angular location. Hence, PNL suppression might be greater for a real operating aircraft.

Atmospheric Attenuation Effects

The PNL suppression may also be increased over that predicted herein because of the conservative atmospheric attenuation correction used in the PNL calculations for this report. Since atmospheric attenuation is greatest at the higher frequencies, the scaled SPL spectra dominated by the higher frequencies should have their PNL values reduced. However, the circular-convergent-nozzle PNL will remain dominated by the lower frequencies since they have significantly higher SPL values.

Additional Noise Suppression Techniques

Perceived noise levels may be further suppressed by the following techniques:

(1) Increasing the atmospheric attenuation by shifting the peak SPL to higher frequencies where the atmospheric absorption is greater has been used to gain increased PNL suppression of jet noise. The multitube nozzle, in part, uses the Strouhal relation

to increase the peak frequency of the jet spectrum by decreasing the individual jet diameter. A similar effect should be possible for the DLS nozzle simply by using a greater number of primary plates, thus decreasing the size of the jet flow coming from each plate. Because the total plate projected area remains the same, the thrust loss should not increase significantly. This concept needs further experimental testing to determine its feasibility.

(2) With an increase in the peak frequency of the jet achieved by using the DLS nozzle, another option becomes available - that of an acoustically absorbent liner in the ejector. Use of this liner may decrease the PNL of the jet an additional 5 to 6 PNdB.

(3) Up to this point, it has been assumed that the jet originates from basically a single nozzle. Installation of the DLS nozzle on the fan jet nozzle of a turbofan engine having coplanar jet exhaust nozzles could result in suppression of both the fan and core jet noise. From an examination of the aerodynamics of the configuration, with the assumption that the fan jet is high pressure and the core jet is low pressure, it would appear that the core jet should not greatly affect the aerodynamics of the DLS nozzle. In fact, the overexpansion in the fan jet caused by the DLS nozzle should cause the core jet to accelerate. If the total pressure of the core jet is large enough, the core jet may become supersonic as it expands from its nozzle. If this occurs, shocks will exist in the core flow within the divergent, lobed section of the DLS nozzle. This should result in lower jet velocity and noise. This concept also needs further experimental investigation to determine its feasibility and the optimum bypass ratio, pressure ratios, and configuration for noise reduction.

Application of DLS Nozzle To Variable-Geometry Engines

One further comment concerning the conversion of the DLS nozzle to a convergent-divergent nozzle for use in supersonic cruise operation seems appropriate here. The basic configuration for this mode of operation is present in the DLS nozzle. Retracting the V-gutter plates and sealing the divergent, lobed section of the nozzle are all that is necessary. Thus, much of the weight added by the DLS nozzle would be offset by its use as the supersonic cruise convergent-divergent nozzle. Subsonic cruise can be accomplished by ducting the convergent nozzle flow through a variable-area or storable ejector with the divergent, lobed section retracted into the ejector wall.

In conclusion, it is apparent that the full potential of the DLS nozzle has not been reached. Additional research and development are needed to explore the preceding suggestions. The suggested application of the DLS nozzle concept to turbofan engines with low-energy core jets seems particularly to warrant this research.

SUMMARY OF RESULTS

A divergent, lobed, suppressor (DLS) nozzle was tested acoustically over a range of nozzle pressure ratios from 1.5 to 4.0. Thrust data were also taken. Results of these experimental small-scale cold-flow tests have been compared with data from a circular, convergent nozzle. The following conclusions can be drawn:

1. Suppression of the jet noise occurred for nozzle pressure ratios of 2.5 to 4.0.
2. Maximum-lobe overall sound pressure level jet noise suppression was 14.6 decibels at a nozzle pressure ratio of 3.5. The thrust loss with the ejector located at the optimum thrust axial position (one primary nozzle throat diameter from the primary nozzle exit) was 2 percentage points greater than the measured thrust loss for the circular convergent nozzle.
3. The free-field, lossless, 90° angular location (sideline) SPL jet noise suppression was 10 decibels with the ejector located at the optimum thrust axial position.
4. The spectral data for the DLS nozzle showed sound pressure level and sound power level suppression of the jet noise at low frequencies.
5. At nozzle pressure ratios above 3.8 and test-stand conditions the DLS nozzle with ejector produced slightly more thrust than the circular, convergent nozzle.
6. The small-scale test data scaled to 15 times test size to simulate a full-size engine nozzle of 1.14-meter diameter showed that perceived noise level suppressions of the order of 12 PNdB are possible with the divergent, lobed, suppressor nozzle. A hard-wall ejector was located 1.33 primary nozzle diameters from the circular-convergent-nozzle throat, and the nozzle pressure ratio was 3.5. The thrust loss would be 2 percent.

Lewis Research Center,
National Aeronautics and Space Administration,
Cleveland, Ohio, December 9, 1974,
505-03.

APPENDIX A

SYMBOLS

c	speed of sound, m/sec
D	diameter, cm
D_t	circular convergent (primary) nozzle throat diameter, cm
F	thrust, N
f	frequency, Hz
h	base cavity step height, cm
OASPL	overall sound pressure level, dB (re 20 $\mu N/m^2$)
P	total pressure, N/m^2
PNL	perceived noise level, PNdB
PWL	sound power level, dB (re 10^{-13} W)
p	static pressure, N/m^2
SPL	sound pressure level, dB (re 20 $\mu N/m^2$)
v	velocity, m/sec
W	power, W
x	axial distance measured from primary nozzle exit or throat station in direction of jet flow, cm
β	microphone angular location measured from upstream (inlet) jet axis (acoustic radiation angle, or directivity), deg
ρ	density, kg/m^3

Subscripts:

c	circular convergent nozzle
DLS	divergent, lobed, suppressor nozzle
e	ejector
exp	experimental
N	nozzle inlet
n	net
p	primary

ref	reference
t	throat
th	theoretical
0	atmospheric

APPENDIX B

DATA REDUCTION EQUATIONS

The detailed equations used in the reduction of the sound data are given herein. The overall sound pressure level (OASPL) was calculated from

$$\text{OASPL} = 10 \log_{10} \sum_{1}^{n} 10^{\left[(\text{SPL}_n)/10\right]}, \quad \text{dB}$$

where

SPL_n 1/3-octave-band SPL value, dB

n 1/3-octave-band-pass filter number

The sound power level (PWL) spectrum was calculated from the sound pressure level spectrum by using the relation PWL = Intensity × Area, or

$$\text{PWL} = 10 \log_{10} \sum_{M=1}^{M=11} \frac{p_n^2}{\rho_0 c_0} \frac{\Delta A_M}{W_{ref}}, \quad \text{dB}$$

where

ΔA_M segment of spherical surface assigned to microphone, m^2

c_0 atmospheric speed of sound, m/sec

M microphone number

p_n sound pressure for any given 1/3-octave-band-pass filter n, N/m^2

ρ_0 atmospheric density, kg/m^3

W_{ref} reference power, 10^{-13} W

The overall sound power level (OAPWL) was calculated by summing the powers, in watts, given by the power spectrum:

$$\mathrm{OAPWL} = 10 \log_{10} \sum_{n=1}^{n} \sum_{M=1}^{M=11} \frac{p_n^2}{\rho_0 c_0} \frac{\Delta A_M}{W_{ref}}$$

The thrust loss was defined as the difference between the ideal net thrust $F_{n,th,c}$ of a circular, convergent nozzle and the measured thrust $F_{n,exp}$ divided by the circular convergent ideal net thrust $F_{n,th,c}$, converted to a percentage. The ideal net thrust was calculated from

$$F_{n,th,c} = w_p v_p + A_p(p_p - p_0)$$

where

w_p calculated primary mass flow rate, kg/sec

v_p calculated flow velocity at circular, convergent nozzle throat, m/sec

A_p primary or circular, convergent nozzle throat area, m^2

p_p calculated primary nozzle throat static pressure, N/m^2 (For Mach numbers less than 1.0, $p_p = p_0$; for Mach numbers greater than 1.0, p_p is 0.528 times the measured nozzle total pressure.)

p_0 ambient pressure, N/m^2

APPENDIX C

SCALING OF COLD-FLOW MODEL TEST DATA TO A FULL-SIZE NOZZLE

The small-scale, cold-flow, sound pressure level test data were scaled to full size to determine the perceived noise level at a 648-meter sideline distance. The diameter of the full-size exhaust nozzle (1.14 m) was 15 times the diameter of the small-scale nozzle. The measured sound pressure levels were scaled with the nozzle area and adjusted for sideline distance by the inverse square law. The frequencies were scaled by the Strouhal relation, fD/v = Constant. Atmospheric attenuation corrections to the scaled-up SPL values were made by the method given in reference 11. The perceived noise levels in PNdB were calculated by the method of reference 11.

In scaling the data, it was necessary to extrapolate the experimental data beyond the 20 000-hertz limit of the acoustic recording and analysis equipment used for the small-scale tests. A dropoff of 2 decibels per 1/3-octave band was assumed. The upper limit of 20 000 hertz in small scale becomes 1333 hertz for the full-size nozzle; therefore, the small-scale data can be used accurately only for estimating the low-frequency (<1333 Hz) full-size acoustic performance.

APPENDIX D

TEMPERATURE EFFECTS ON DIRECTIVITY AND SUPPRESSION

The maximum-lobe, overall sound pressure level of the circular, convergent nozzle at cold-flow conditions (figs. 4(c) to (f)) occurred just off the jet axis. Correcting all OASPL levels for sideline distance attenuated the levels so that the 90° location (minimum sideline distance) is maximum. Since the OASPL of the DLS nozzle with ejector was nearly independent of directivity angle, the sideline suppression was not affected by the maximum-lobe OASPL of the circular, convergent nozzle. Unpublished NASA data show that for a hot jet the maximum-lobe angular location for the circular, convergent nozzle moves away from the jet axis (β becomes smaller) and that the sideline noise may be dominated by the maximum-lobe OASPL (because of the smaller correction due to the shorter distance).

Unpublished NASA data also show that the maximum-lobe location for the DLS nozzle shifts only slightly between cold and hot tests. The large shift in maximum-lobe location of the circular, convergent nozzle with temperature compared with the smaller shift of the DLS nozzle indicates that the suppressor nozzle may give greater sideline suppression for hot flow than those shown in figure 7, herein, for cold flow.

REFERENCES

1. Lighthill, M. J.: Jet Noise. AIAA J., vol. 1, no. 7, July 1963, pp. 1507-1517.
2. von Glahn, U. H.: Correlation of Total Sound Power and Peak Sideline OASPL from Jet Exhausts. AIAA Paper 72-643, June 1972.
3. Eldred, Kenneth M.; White, Robert W.; Mann, Myron A.; and Cuttis, Miltiades G.: Suppression of Jet Noise with Emphasis on the Near Field. Western Electro-Acoustic Lab., Inc. (ASD-TDR-62-578), 1963, pp. 101-102.
4. Huff, Ronald G.; and Groesbeck, Donald E.: Splitting Supersonic Nozzle Flow into Separate Jets by Overexpansion into a Multilobed Divergent Nozzle. NASA TN D-6667, 1972.
5. Huff, Ronald G.; and Groesbeck, Donald E.: Geometric Factors Affecting Noise Suppression and Thrust Loss of Divergent-Lobe Supersonic Jet Noise Suppressor. NASA TM X-2820, 1973.
6. Gray, V. H.; Gutierrez, O. A.; and Walker, D. Q.: Assessment of Jets as Acoustic Shields by Comparison of Single and Multitube Suppressor Nozzle Data. AIAA Paper 73-1001, Oct. 1973.
7. Olsen, W. A.; Gutierrez, O. A.; and Dorsch, R. G.: The Effect of Nozzle Inlet Shape, Lip Thickness, and Exit Shape and Size on Subsonic Jet Noise. AIAA Paper 73-187, Jan. 1973.
8. Martlew, D. L.: Noise Associated with Shock Waves in Supersonic Jets. Aircraft Engine Noise and Sonic Boom. AGARD-CP-42, Advisory Group for Aerospace Research and Development, 1969, pp. 7-10.
9. Callagahn, Edmund E.; and Coles, Willard D.: Far Noise Field of Air Jets and Jet Engines. NACA TR 1329, 1957.
10. Woodward, Richard P.; and Minner, Gene L.: Low-Frequency Rear Quadrant Noise of a Turbojet Engine with Exhaust Duct Muffling. NASA TM X-2718, 1973.
11. Noise Standards: Aircraft Type Certification. Federal Aviation Regulations, vol. III, Part 36, 1969.

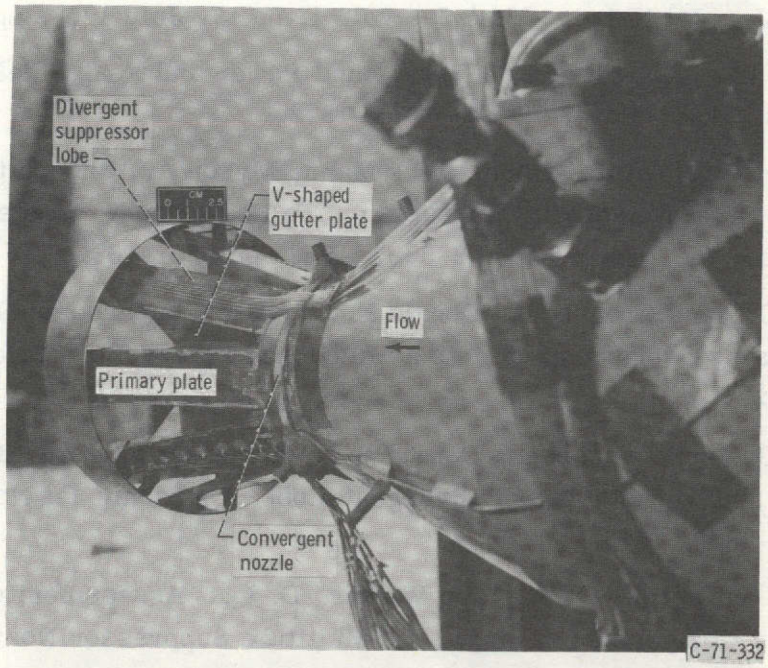

(a) Nozzle viewed in direction of jet efflux.

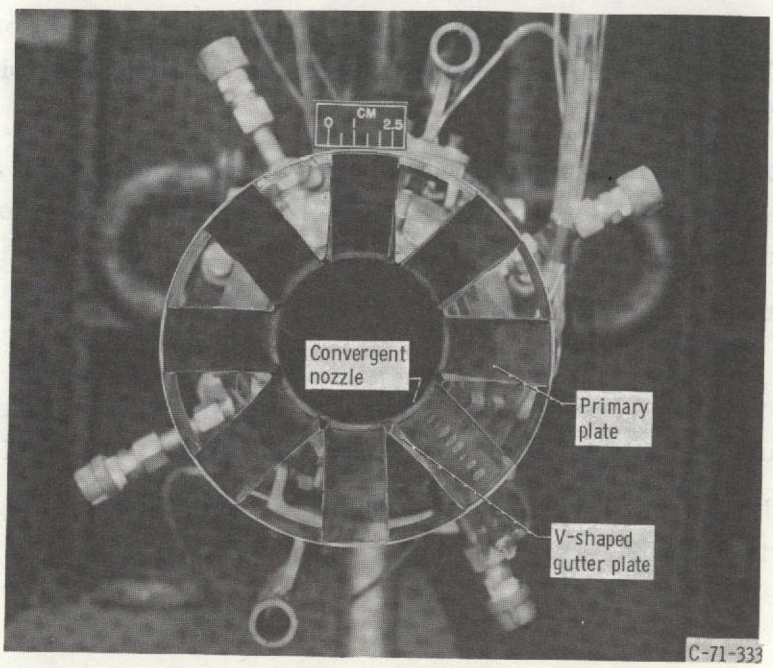

(b) Rear view of nozzle.

Figure 1. - Divergent, lobed nozzle as installed in cold flow test facility. (Original configuration is shown. For this test the modified configuration illustrated in fig. 2 was used.)

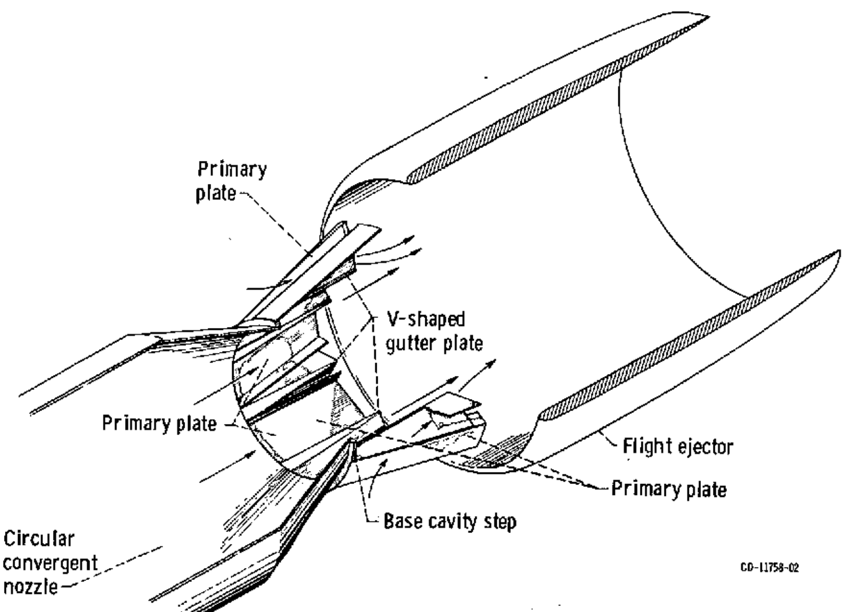

(a) Isometric view.

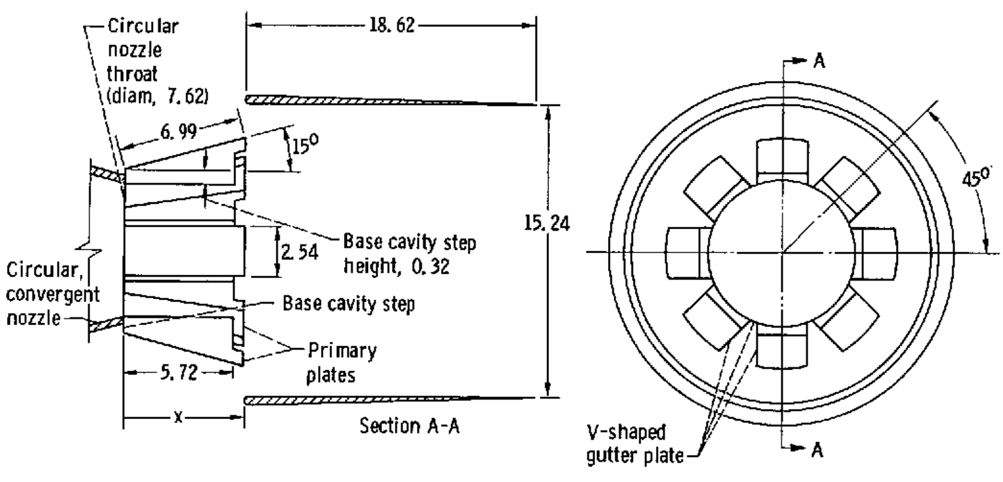

(b) Dimensions (in centimeters).

Figure 2. - Divergent, lobed, suppressor nozzle test configuration with ejector installed.

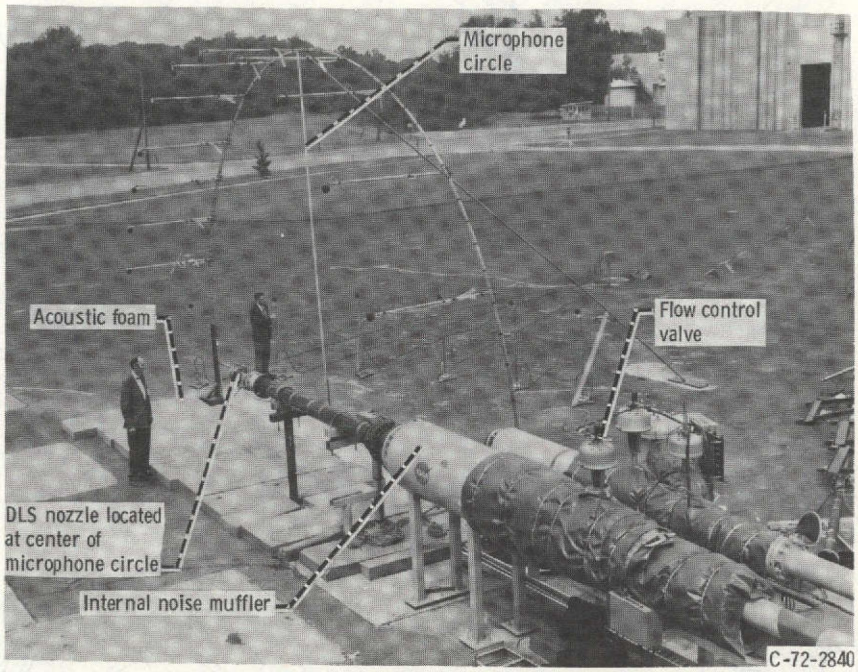

Figure 3. - Cold-flow, jet noise, test facility.

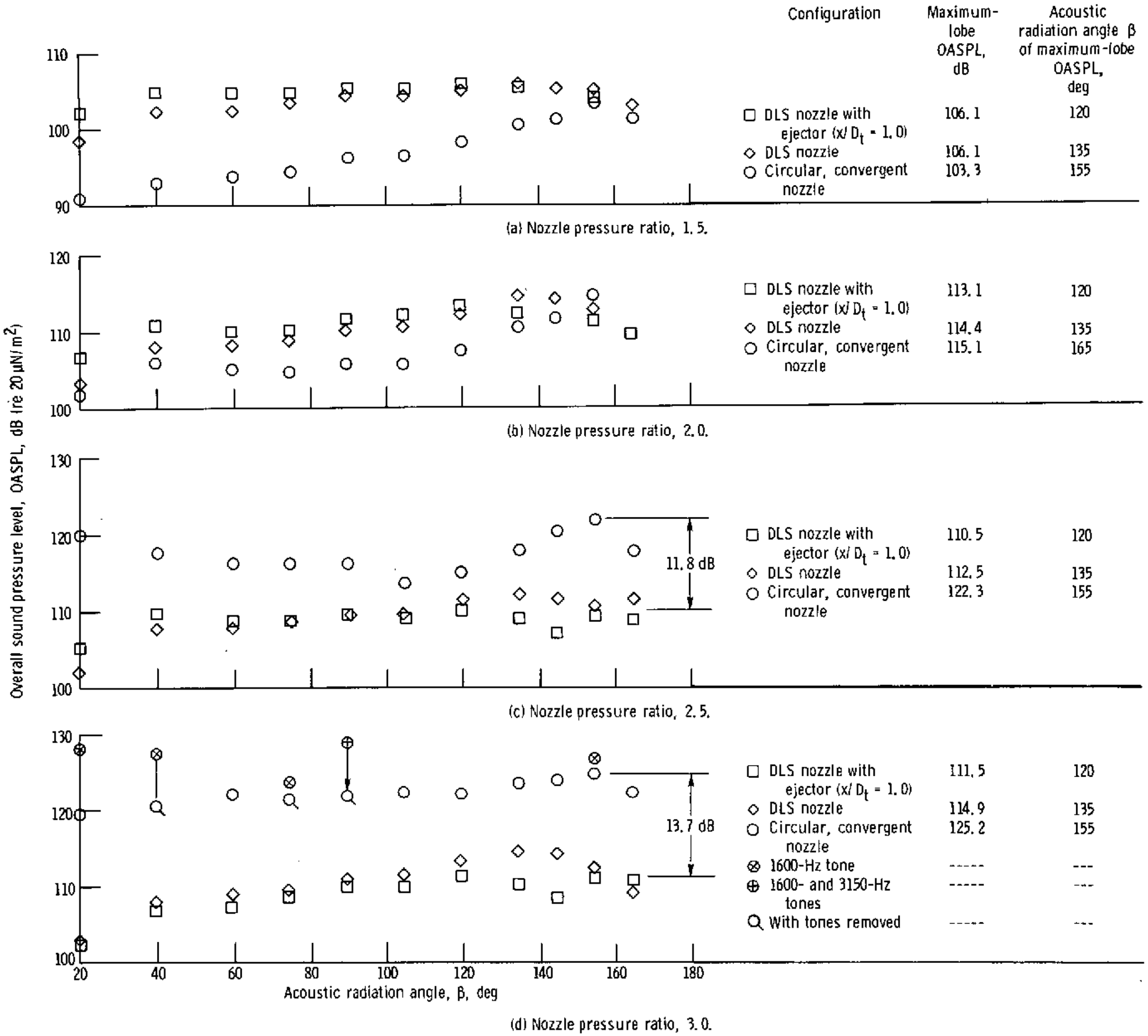

Figure 4. - Comparison of overall sound pressure level angular distributions for divergent, lobed, suppressor nozzle with those for circular, convergent nozzle. Microphone radius, 4.57 meters; cold-flow, free-field, lossless data.

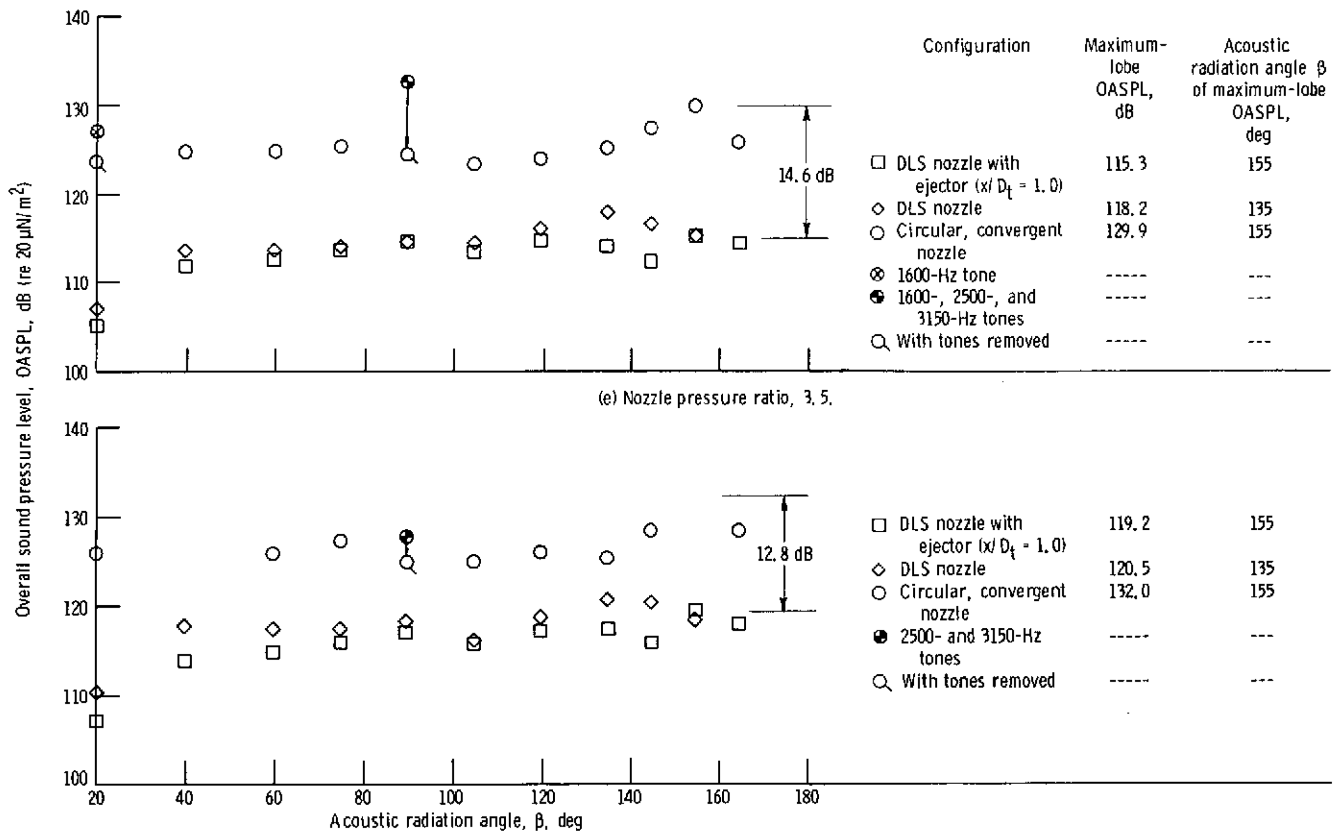

(f) Nozzle pressure ratio, 4.0.

Figure 4. - Concluded.

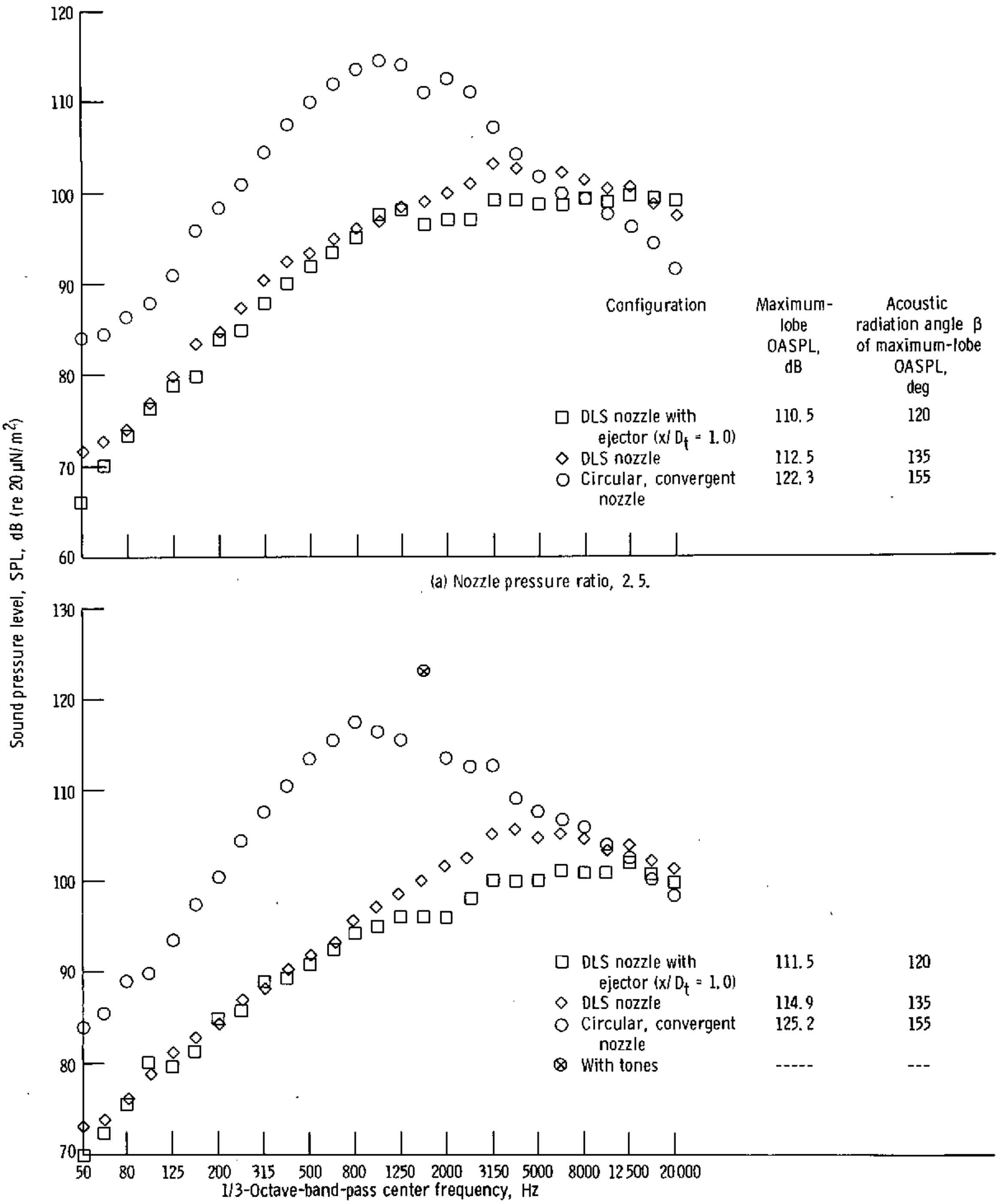

(a) Nozzle pressure ratio, 2.5.

(b) Nozzle pressure ratio, 3.0.

Figure 5. - Comparison of maximum-lobe sound pressure level spectra for divergent, lobed, suppressor nozzle with those for circular, convergent nozzle. Microphone radius, 4.57 meters; cold-flow, free-field, lossless data.

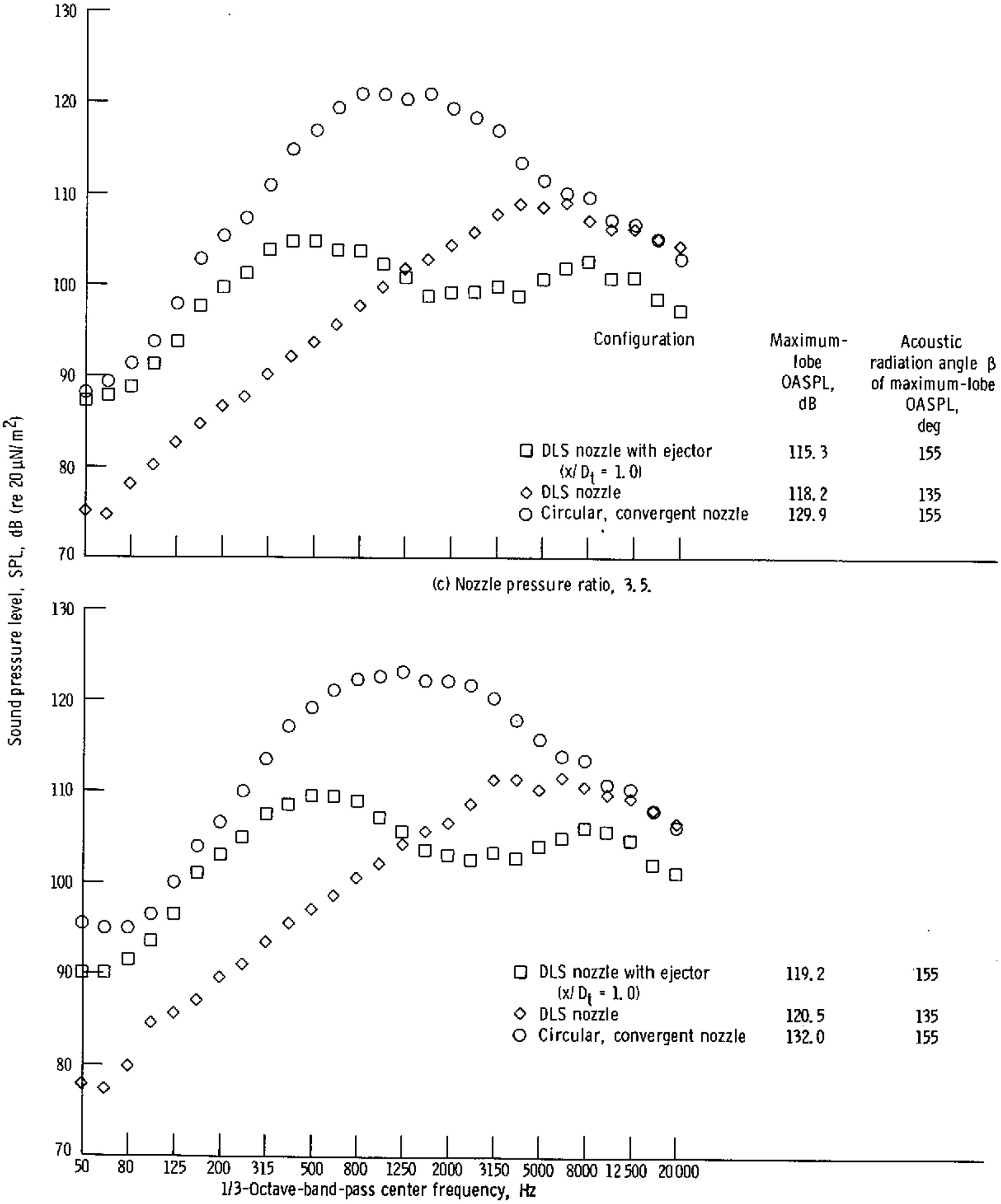

(c) Nozzle pressure ratio, 3.5.

(d) Nozzle pressure ratio, 4.0.

Figure 5. - Concluded.

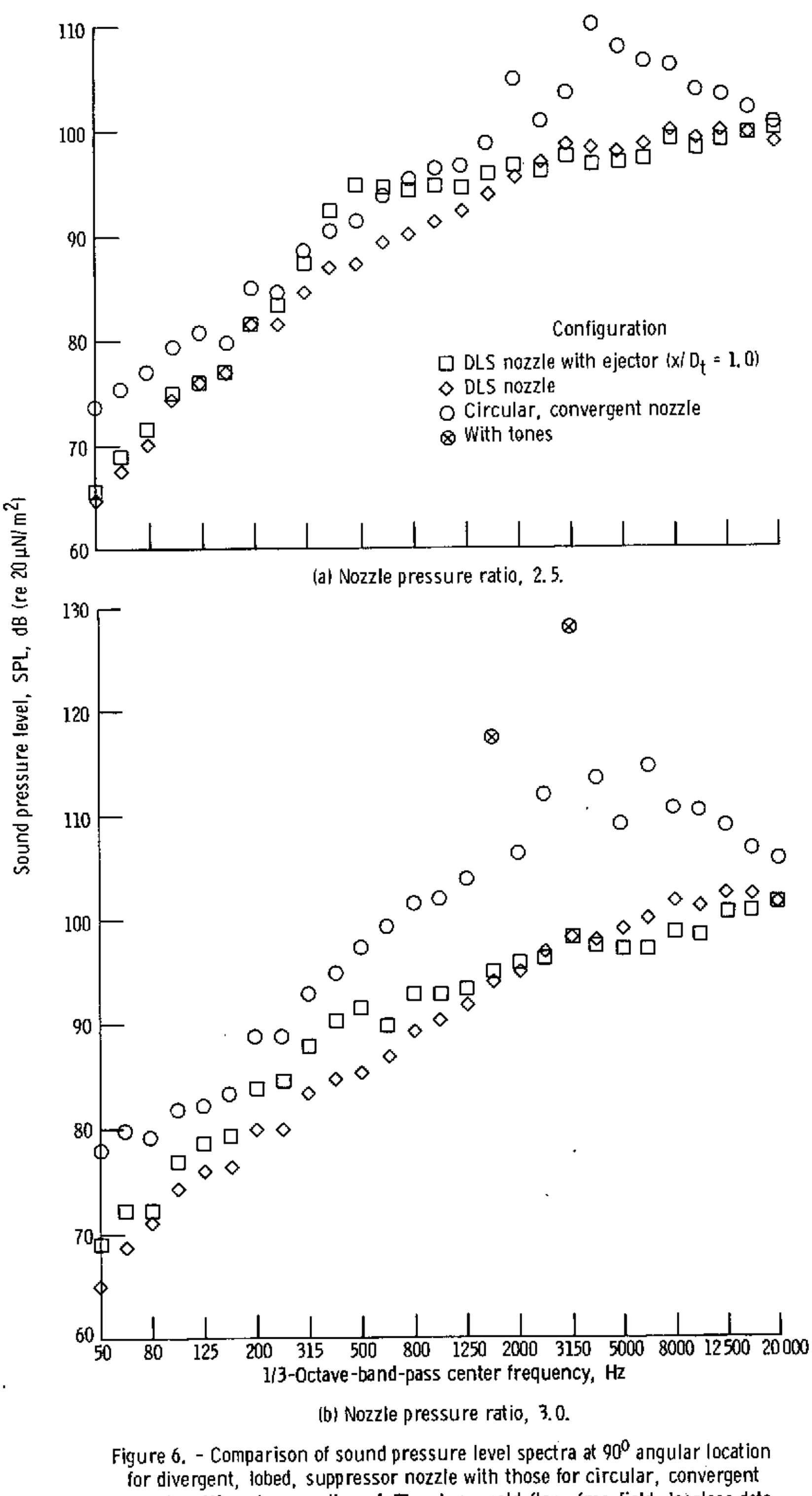

Figure 6. - Comparison of sound pressure level spectra at 90° angular location for divergent, lobed, suppressor nozzle with those for circular, convergent nozzle. Microphone radius, 4.57 meters; cold-flow, free-field, lossless data.

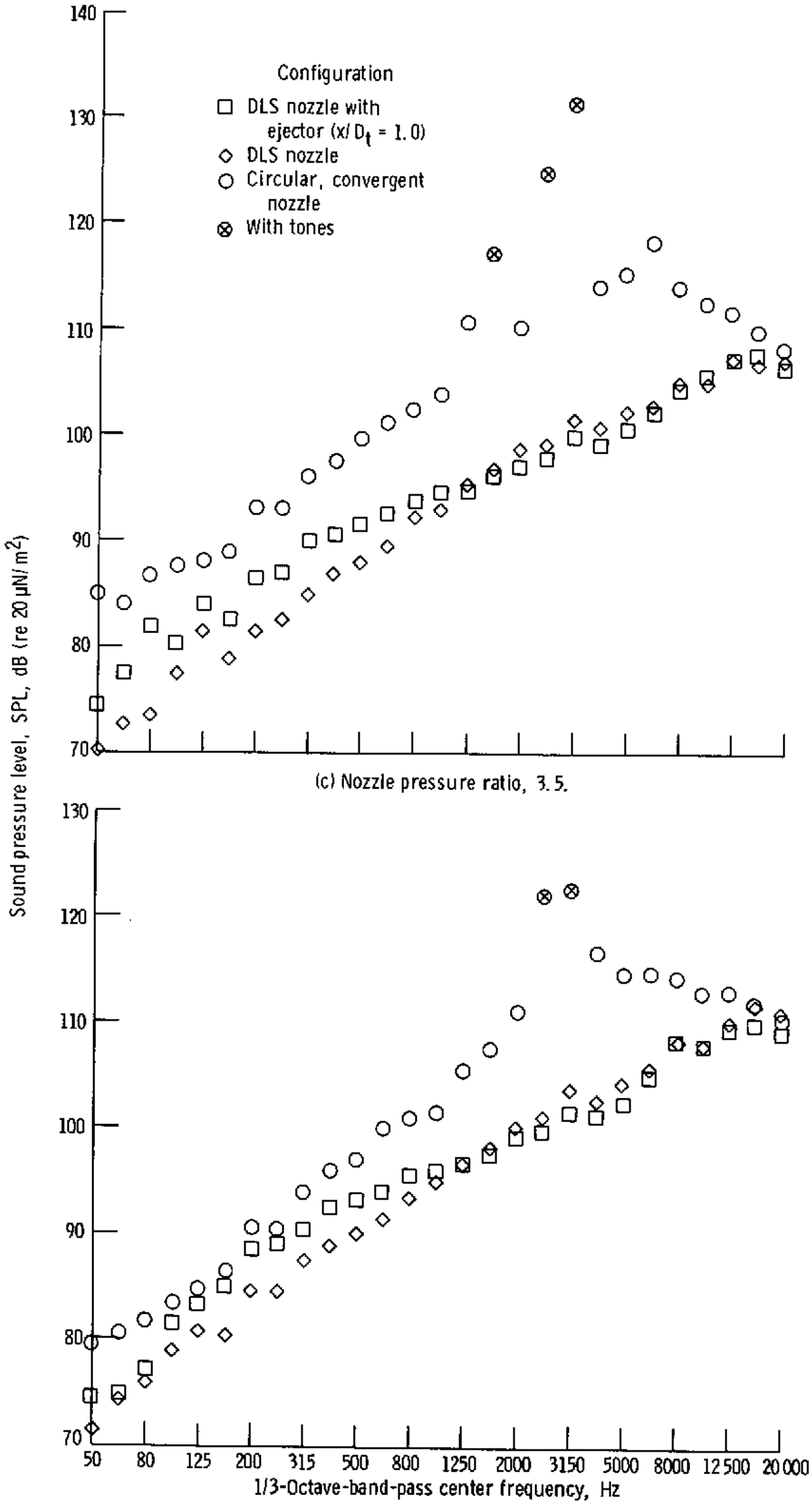

(d) Nozzle pressure ratio, 4.0.

Figure 6. - Concluded.

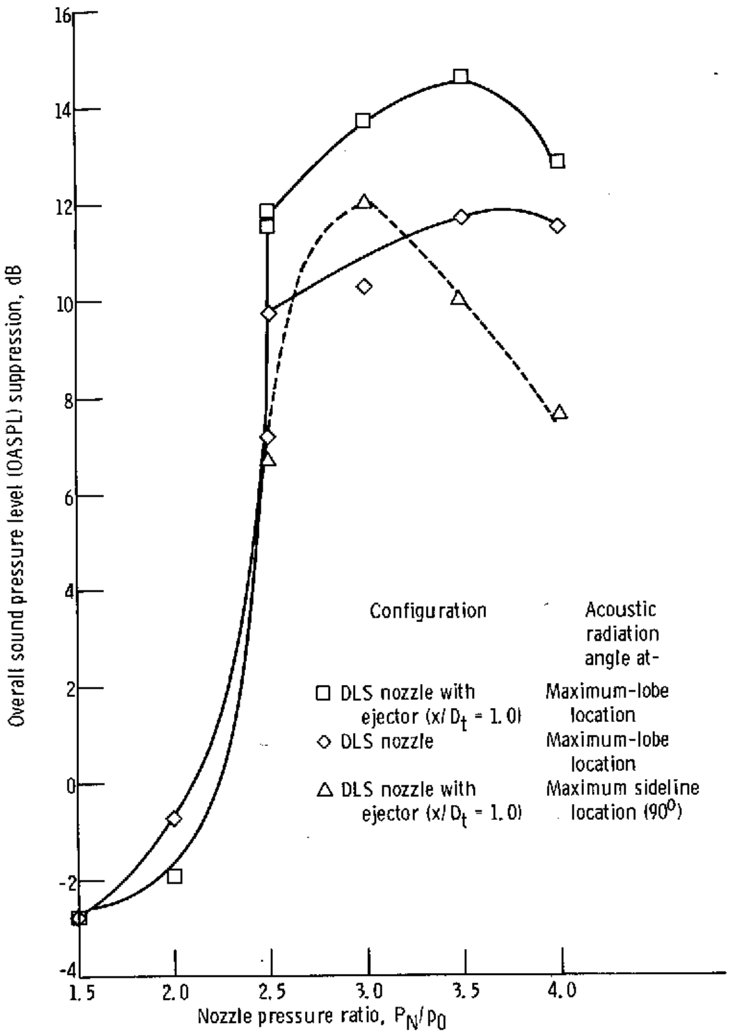

Figure 7. - Noise suppression by divergent, lobed, suppressor nozzle with and without ejector at optimum thrust position (x/D_t = 1.0).

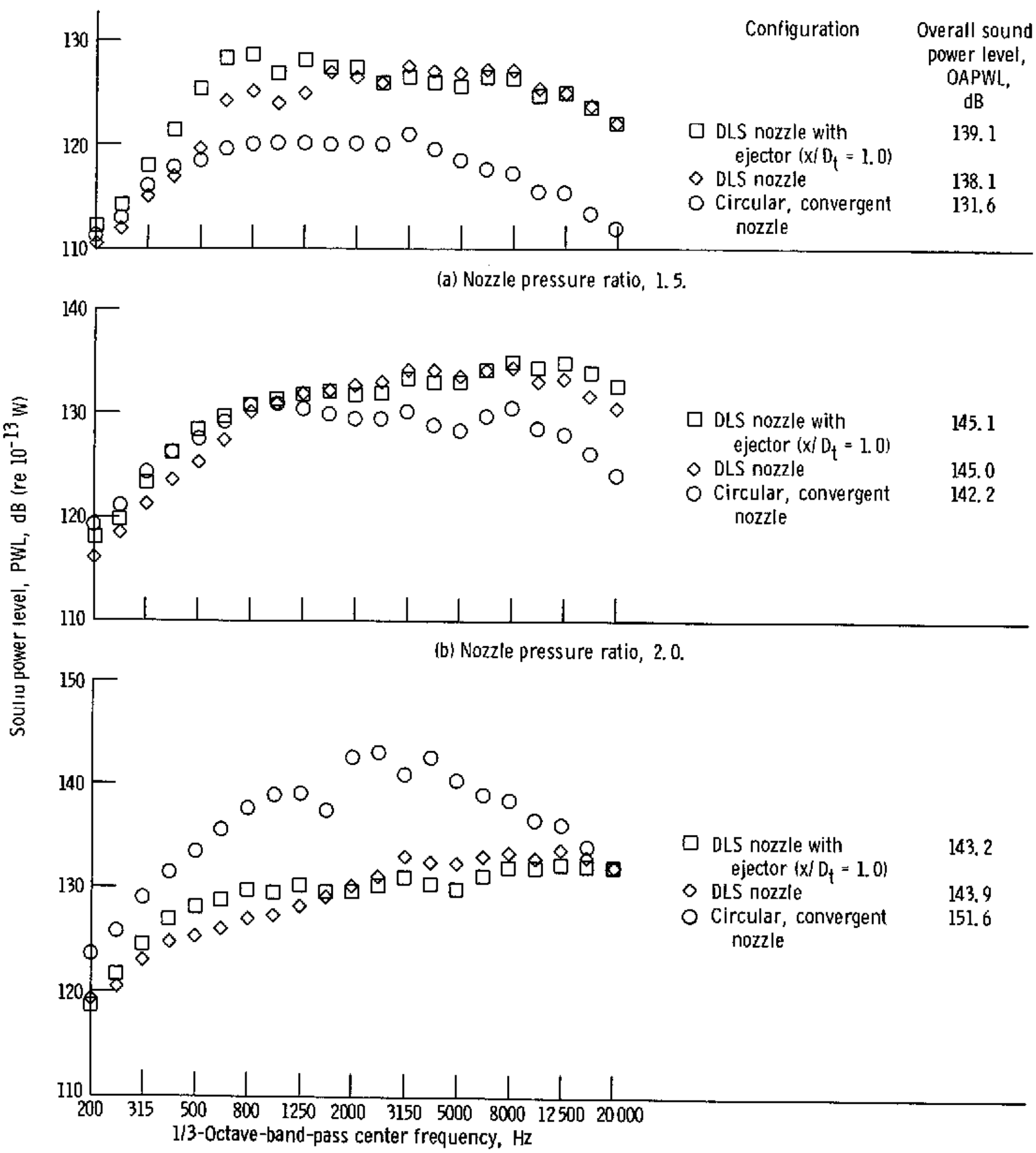

Figure 8. - Comparison of sound power level spectra for divergent, lobed, suppressor nozzle with those for circular, convergent nozzle.

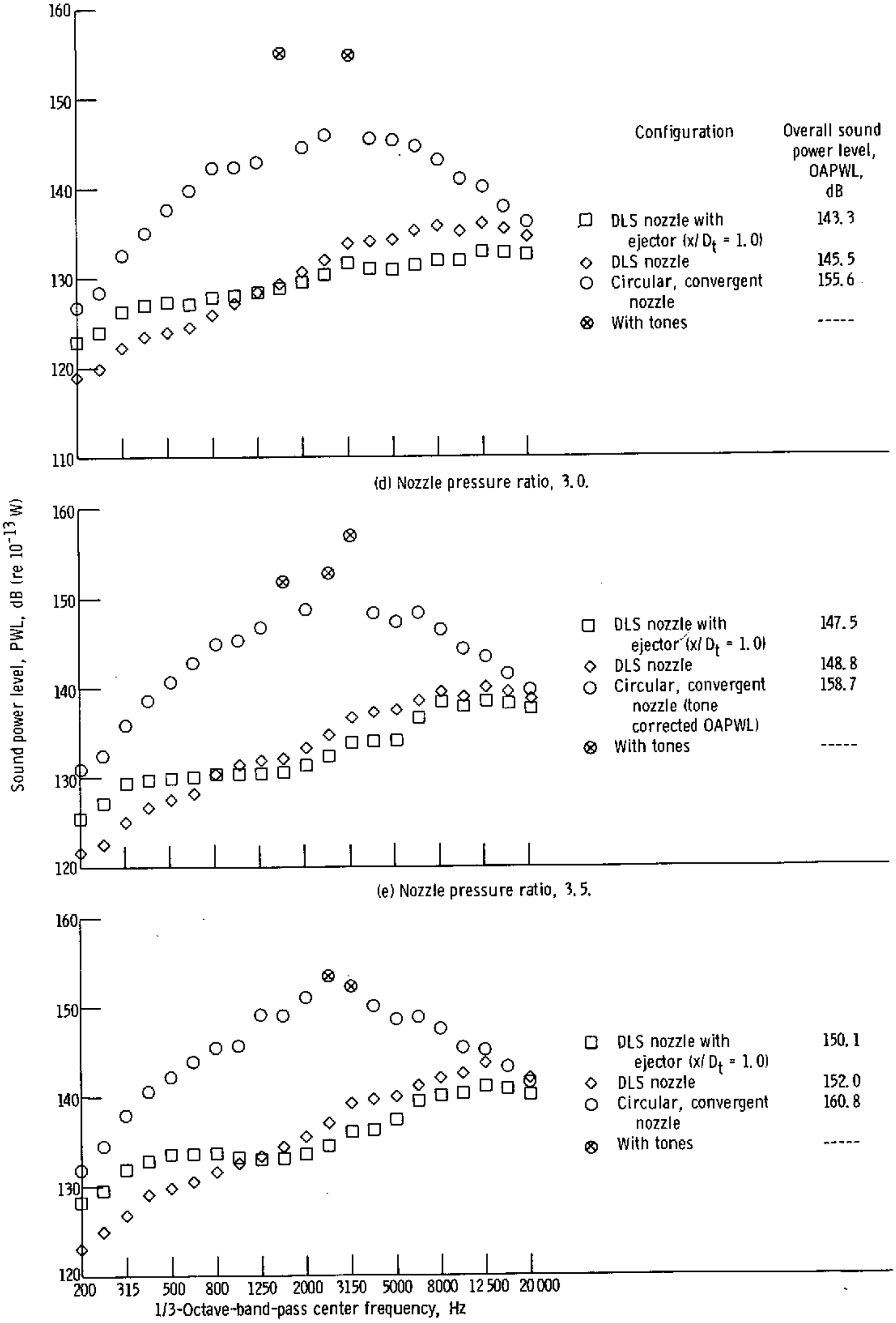

(d) Nozzle pressure ratio, 3.0.

(e) Nozzle pressure ratio, 3.5.

(f) Nozzle pressure ratio, 4.0.

Figure 8. - Concluded.

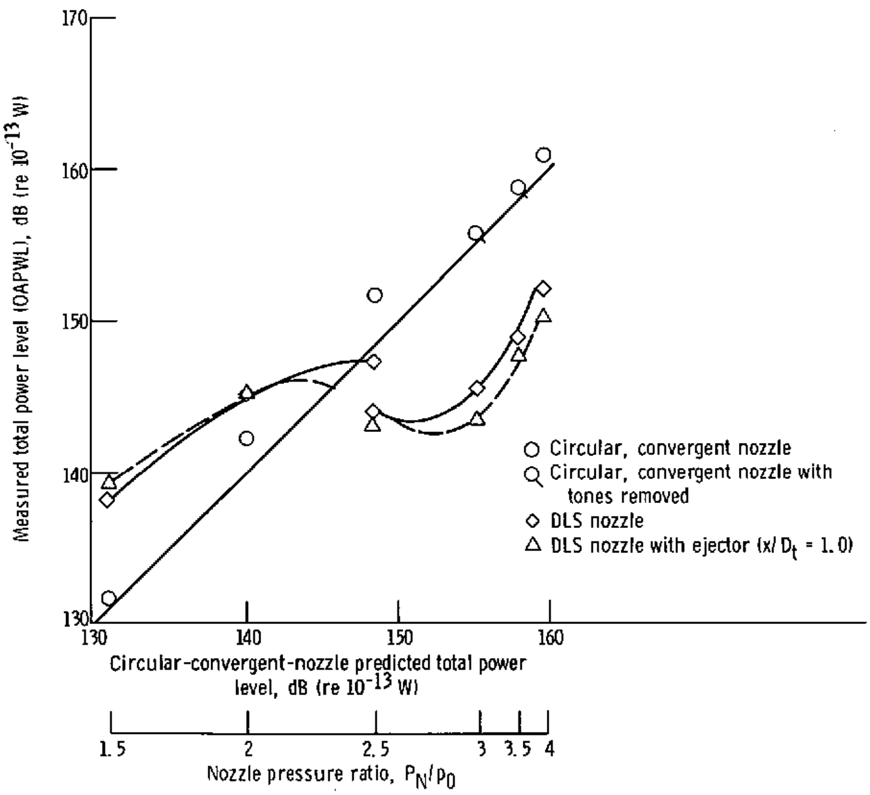

Figure 9. - Comparison of measured total power level of divergent, lobed, suppressor nozzle and circular, convergent nozzle with circular, convergent nozzle total power level predicted by method of reference 2.

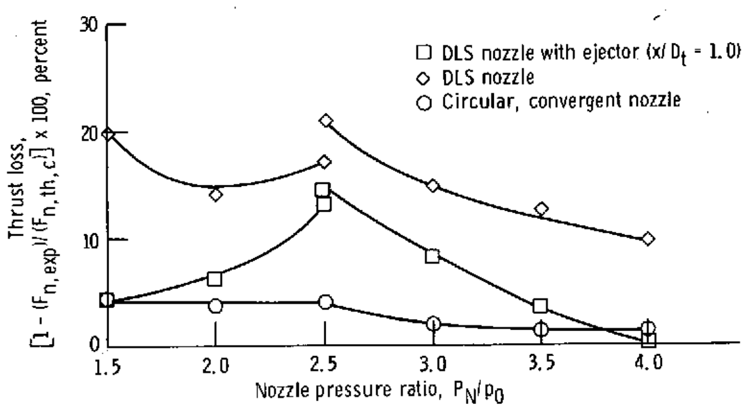

Figure 10. - Thrust loss of divergent, lobed, suppressor nozzle as function of nozzle pressure ratio. Ejector located at optimum thrust position.

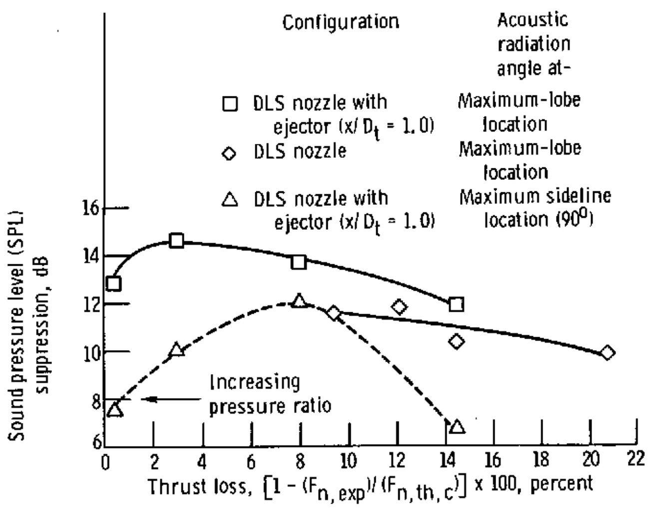

Figure 11. - Noise suppression of divergent, lobed, suppressor nozzle as function of thrust loss. Nozzle pressure ratio range, 2.5 to 4.0.

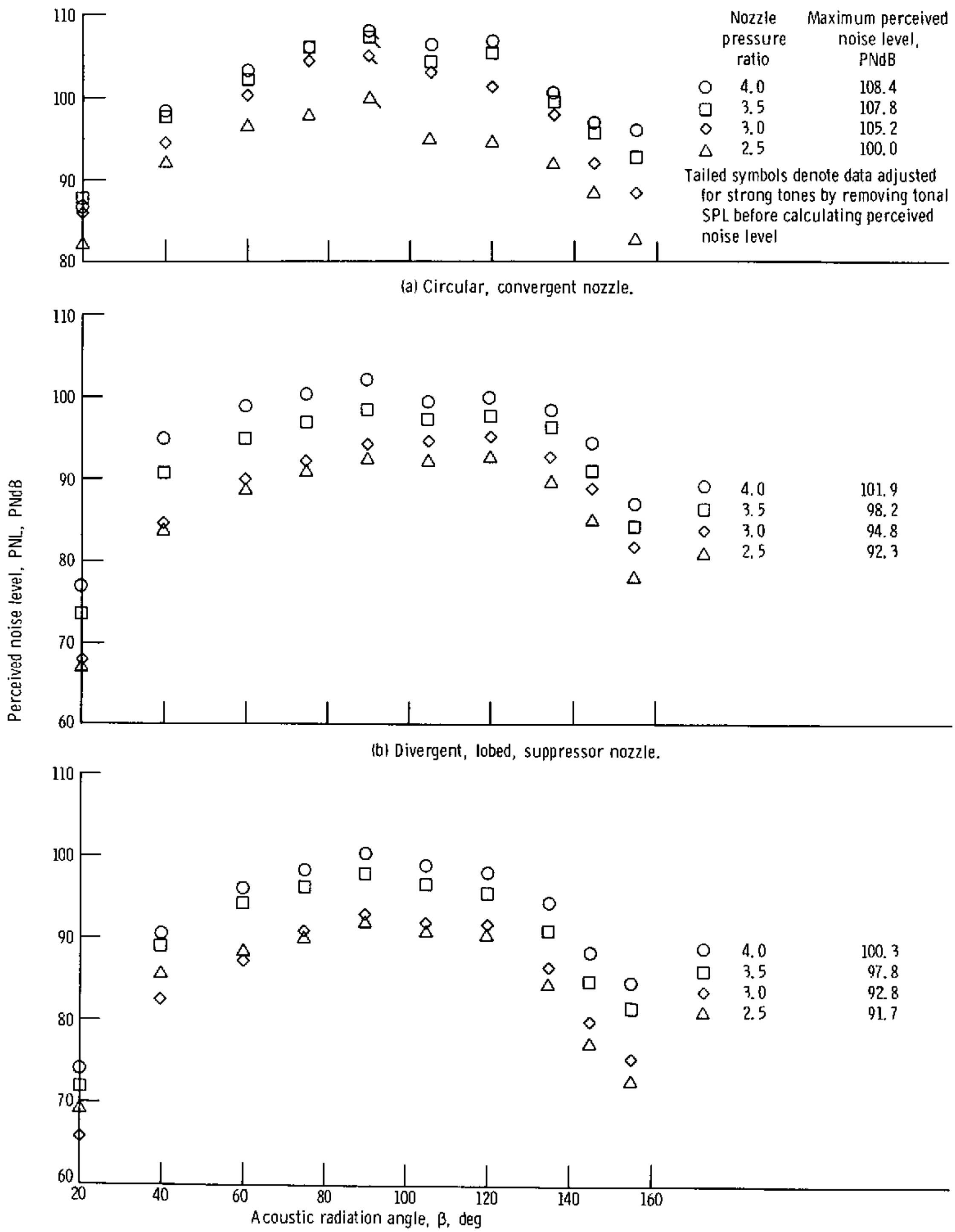

(c) Divergent, lobed, suppressor nozzle with ejector at $x/D_t = 1.0$.

Figure 12. - Estimated perceived noise level at 648-meter sideline for full-size (1.14 m diameter) nozzle for various pressure ratios. Scale factor, 15 times model size; atmospheric attenuation included.

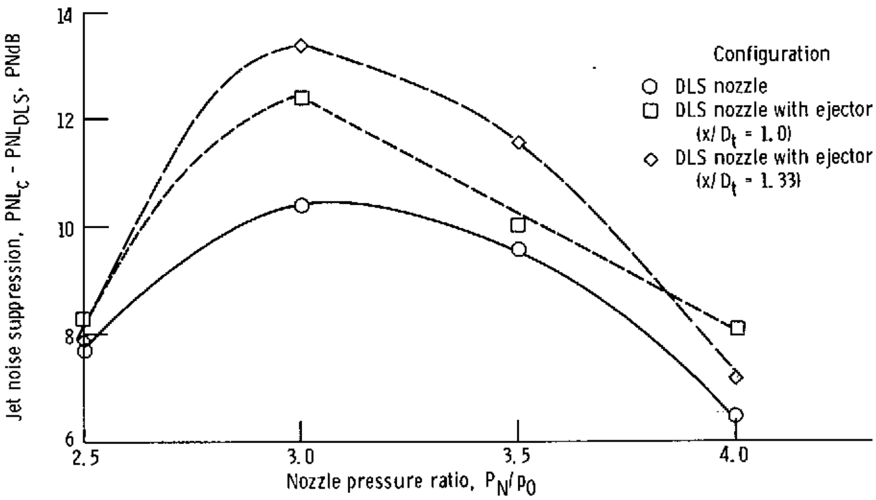

Figure 13. - Perceived noise level suppression at 648-meter sideline for full-size (1.14 m) nozzle Data scaled from small-scale, cold-flow model tests. Scale factor, 15 times model size.

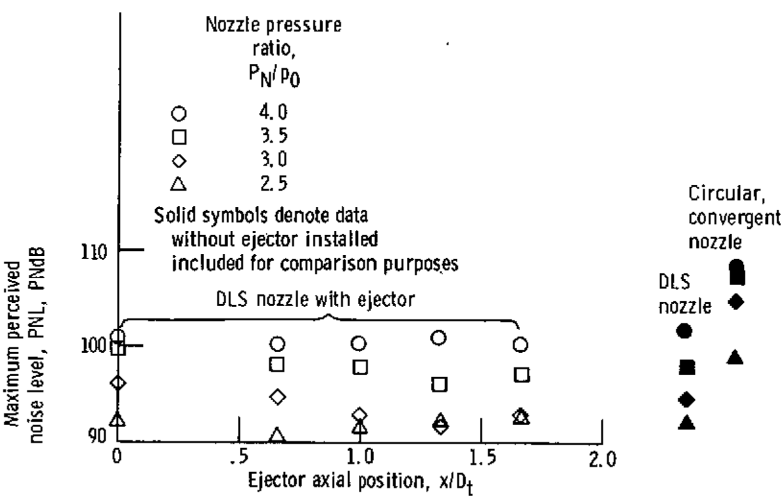

Figure 14. - Maximum sideline perceived noise level of full-size, divergent, lobed, suppressor nozzle at 648-meter sideline.